Polarization bremsstrahlung from xenon atoms and clusters: A cooperative effect contribution

E. V. Gnatchenko, A. N. Nechay, V. N. Samovarov, and A. A. Tkachenko
B. Verkin Institute for Low-Temperature Physics and Engineering, National Academy of Sciences of Ukraine, 47 Lenin Avenue, Kharkiv 61103, Ukraine
(Received 8 April 2010; published 8 July 2010)

Polarization bremsstrahlung (PBS) on scattering of 0.7-keV electrons on Xe clusters of various size is studied experimentally. The PBS spectrum is found to change upon passage from Xe gas to clusters. There takes place a shift of the PBS maximum to lower energies and a narrowing of its spectral profile. Calculations of the PBS cross section are made for Xe clusters in two models: one takes into account dielectric permeability of the environment of an emitting dipole and the other takes into consideration the frequency dependence of the dipole damping. The calculated curves fit the experimental PBS spectra well and account for the spectral changes occurring upon transition from the gas to the clusters. It is found that cooperative effects in a solid strongly influence the PBS spectrum.

DOI: 10.1103/PhysRevA.82.012702 PACS number(s): 34.80.−i, 78.70.−g, 78.67.Bf

I. INTRODUCTION

Bremsstrahlung, which arises in the scattering of electrons by atoms and condensed media, has been one of the fundamental problems of interaction between electrons and substances since at least the beginning of the 20th century. In the 1970s, the bremsstrahlung physics underwent a "rebirth." It was established that, in the process of scattering of a charged particle by a target, the bremsstrahlung (BS) is formed in two essentially different ways. The first mechanism had been studied rather thoroughly earlier and implies *ordinary (static) bremsstrahlung* (OBS) resulting from deceleration of a charged particle in the static field of the target accompanied by the emission of photons. According to the other mechanism that was found later, the continuous spectrum photons are emitted not by the scattered particle but by the target atoms as a result of their dynamic polarization in an alternating field of the incident particle. The bremsstrahlung formed in the latter way was given the name *polarization bremsstrahlung* (PBS). OBS and PBS spectra not only differ in the mechanisms of their formation (in particular, the PBS does not need any deceleration of the electron) but also have different dependencies on frequency, radiation angle, mass, and energy of the incident particle. It should also be noted that the OBS is formed at small aiming distances from the target, while the PBS is formed at greater ones. The latter implies a possibility of cooperative effects in the medium that should influence the PBS formation.

We would like to note that the PBS was first predicted theoretically [1] and before long was confirmed in BS experiments on scattering of electrons by Xe atoms [2]. The success was in large measure caused by using as the gaseous target a supersonic jet of Xe atoms which has a sharp boundary with the vacuum [3]. For the time being, PBS has been studied experimentally for electrons scattered by atoms of Ar, Kr, Xe [4–6], and Ba [7] and by a number of solid targets of rare-earth elements [8,9]. Theoretical study of PBS is rather well developed: for example, in Refs. [10–12] the influence of number of atoms in metallic clusters as well as of incident electron energy on amplitude and radiation angle of PBS scattering is discussed. For now, however, there are no published data reporting the observation of spectral differences in PBS spectra from atoms, clusters, and solids of one and the same element.

The organization of an experiment for obtaining such data is rather difficult for two reasons. First, one should study PBS for various targets, from atoms to clusters, in one experimental cycle. Second, the highest PBS intensity is expected to be observed from multielecron atoms in the spectral region of their giant absorption resonances, that is, in the hard-to-reach ultrasoft x-ray spectral region [13]. It is in this spectral range that the atoms have a strong dipole dynamic polarizability, which is responsible for the high values of PBS intensity. For the Xe atom the relevant spectral region is near 100 eV. Some additional difficulty arises from BS radiation overlapping with a number of characteristic lines, which makes it more difficult to single out and analyze the continuous PBS spectrum.

The gas jet technique for obtaining rare-gas atom-cluster targets allows one to overcome the mentioned difficulties by taking the following advantages:

(i) By varying gas parameters at the nozzle entrance, it is possible to change the target type from atomic to cluster and to vary gradually the size and density of clusters in the jet.

(ii) It is possible to have the generated radiation directly inside the x-ray spectrometer without using optical windows and differential evacuation systems.

(iii) The sharp boundary of the atom-cluster jet allows the gun to be placed near the jet, which makes it possible to excite the target by bombarding it with an electron beam of high current density and relatively small electron energy of approximately 500 eV.

The present paper is devoted to the comparative study of PBS for intermediate-energy electrons (0.7 keV) scattered by atomic and cluster supersonic jets of xenon. The concentration and size of clusters in the jet target was changed by varying temperature and pressure at the entrance to the supersonic nozzle. The spectra were measured in the photon energy range 80–180 eV.

The paper presents the experimental PBS spectra obtained upon passage from the atomic target to the cluster target. The variation in PBS spectrum effective width is traced upon cluster growth. It is found that as the atom number increases in a cluster the PBS maximum shifts toward the lower energies, while the effective PBS profile width decreases.

The obtained experimental data are compared with the results of model calculations of the PBS spectrum performed

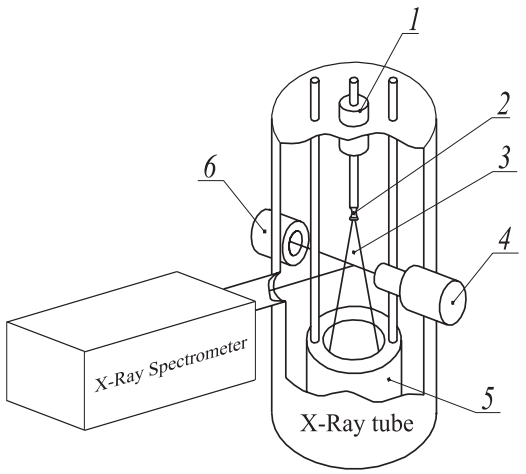

FIG. 1. Schematic view of the experimental setup: 1, heat exchanger; 2, supersonic conic nozzle; 3, supersonic gas jet; 4, electron gun; 5, cryogenic pump; 6, Faraday cylinder.

for two situations: (1) the emitting center is in a medium characterized by some dielectric permeability or (2) there is some retardation of the interaction between the emitting dipole and the medium. The model spectra are in good agreement with the experimental data, evidencing that some solid-state cooperative effects are responsible for the observed changes in the PBS spectra.

II. EXPERIMENT

A. Experimental setup

The experimental method used to study bremsstrahlung from intermediate-energy electrons scattered by atomic jets was previously presented in Refs. [4,14]. The experimental setup (see Fig. 1) consists of an x-ray tube with a supersonic gas jet as the anode and an x-ray spectrometer. The working principle of the setup is as follows. The gas to be investigated is directed to a heat exchanger to acquire its temperature, T_0. The temperature was varied within the range $T_0 = 180-500$ K, and the gas pressure at the nozzle entrance was chosen to be 0.3, 0.6, and 1 bar. The supersonic conical nozzle forms a jet that flows adiabatically into a vacuum chamber. The diameter of the nozzle throat is 0.3 mm, the nozzle length is 10 mm, the area ratio of the exit section to the throat is 59.3, and the cone angle is 9.5°. To continuously evacuate the gas jet, a cryogenic liquid-hydrogen-cooled pump was used.

In certain jet flow regimes, homogeneous condensation of the gas occurs. At first, liquid nanodroplets are formed inside the nozzle and become cool due to their interaction with the atomic component of the jet and then solidify. At a distance of several millimeters from the nozzle exit, the process of formation of solid rare-gas clusters is completed. The cluster temperature is nearly 70 K for xenon and nearly 40 K for argon.

An electron beam crosses the rare-gas jet at a distance of 10 mm from the nozzle exit section. The energy of electrons is 0.7 keV, and the electron current is constant and equal to 20 mA.

Radiation that arises upon interaction of electrons with an atomic or cluster target passes through the entrance slit of the x-ray spectrometer and is registered by a proportional counter filled with methane up to a pressure of 1.5×10^4 Pa. The counter window is made of a nitrocellulose film. Differential BS spectra are measured, and the solid angle of radiation collection is 1.7×10^{-3} sr. The spectral resolution is 1 Å. The angle between the incident electrons and the analyzed photons is 97°.

Methodical studies demonstrate that under constant experimental conditions the BS intensities from atomic Ar, Kr, and Xe jets remain stable over time within an experimental error of 10%. The experiments are carried out in the regime of single collisions. This was evidenced by observation of a linear dependence of BS intensity on electron beam current in the range 5–50 mA.

B. PBS profile extraction

Since the measured spectra are a superposition of PBS and OBS spectra, there was an additional task to correctly extract the true PBS profile. One also had to take into consideration the spectral efficiency of the x-ray spectrometer.

To determine the device spectral efficiency, a technique was used which consisted of comparing the measured and the calculated spectral dependencies of BS resulting from electrons scattered by Ar atoms. Argon was chosen as the target because in our spectral range, 80–180 eV, the PBS intensity from Ar atoms is negligibly small and the Ar characteristic lines are very weak. The experimentally measured quantity was the number of pulses per second $N_{\mathrm{Ar}}(\omega)$, which is proportional to the number of quanta emitted within a frequency range of $\Delta\omega$ from the excitation spot of the jet. Provided that the radiant flux is formed solely by OBS, the following relation can be written:

$$k(\omega)N_{\mathrm{Ar}}(\omega) = \frac{d\sigma(\omega)_{\mathrm{OBS}}}{d\omega}, \tag{1}$$

where $\frac{d\sigma(\omega)_{\mathrm{OBS}}}{d\omega}$ is the differential cross section of OBS from Ar atoms, and $k(\omega)$ is the spectrometer efficiency taken in relative units. Since the OBS cross section follows the $1/\omega$ dependence with a high degree of accuracy, as is known [1], the following holds:

$$k(\omega)N_{\mathrm{Ar}}(\omega) = \frac{A}{\omega}, \tag{2}$$

where the coefficient A takes into account the atomic constants which determine the absolute value of OBS cross section. This allowed us to calculate the device spectral efficiency $k(\omega)$.

In the case of Xe, when there is a superposition of PBS and OBS spectra, the $k(\omega)$ dependence is experimentally measured and thus we have

$$k(\omega)N_{\mathrm{Xe}}(\omega) = \frac{d\sigma(\omega)_{\mathrm{PBS}}}{d\omega} + \frac{d\sigma(\omega)_{\mathrm{OBS}}}{d\omega}, \tag{3}$$

where $\frac{d\sigma(\omega)_{\mathrm{PBS}}}{d\omega}$ is the PBS differential cross section.

By multiplying the left- and right-hand sides of Eq. (3) by ω and taking into account formula (2), we arrive at

$$\omega k(\omega)N_{\mathrm{Xe}}(\omega) = \omega\frac{d\sigma(\omega)_{\mathrm{PBS}}}{d\omega} + \mathrm{const}. \tag{4}$$

Equation (4) allowed us to extract the PBS profile in coordinates $\omega\frac{d\sigma(\omega)_{\rm PBS}}{d\omega}$ versus ω from the measured $N_{\rm Xe}(\omega)$ data. The value of $\omega\frac{d\sigma(\omega)_{\rm PBS}}{d\omega}$ is proportional to the PBS spectral power and is given hereafter in relative units. It should be noted that in the above coordinates the OBS differential cross section is constant and therefore does not affect the PBS profile.

C. Cluster size determination

The average number of atoms in a Xe cluster was determined by using the relations of Hagena [15], which have been confirmed many times in the experimental study of the structure of rare-gas clusters [16]:

$$\langle N\rangle = 2.94\times 10^{-6}(\Gamma^*)^{2.35}, \tag{5}$$

where

$$\Gamma^* = \left[K\frac{P_0}{T_0^{2.456}}\left(0.74\frac{d}{\tan\beta}\right)^{0.85}\right]. \tag{6}$$

Here $\langle N\rangle$ is the average number of atoms in a cluster, Γ^* is the Hagena parameter, K is a coefficient characteristic of a certain gas ($K = 5500$ for Xe), P_0 (mbar) and T_0 (K) are the pressure and temperature of the gas at the nozzle entrance, d is the nozzle diameter (μm), and β is the half opening angle of the nozzle.

It should be noted that relation (5) having an index of power of 2.35 is only valid for the Hagena parameter value range $2000 \leqslant \Gamma^* \leqslant 20\,000$, which corresponds in our cases to the experimental conditions with $0.6 \leqslant P_0 \leqslant 1$ bar and $180 \leqslant T_0 \leqslant 300$ K. In accordance with Eqs. (5) and (6), the number of atoms in the cluster varies from several tens to $\sim 8.5\times 10^3$ in our experiments. For temperatures near 500 K and pressure of 0.6 bar (corresponding to $\Gamma^* \sim 600$), Eq. (5) reads

$$\langle N\rangle = 4.62\times 10^{-4}(\Gamma^*)^{1.64}. \tag{7}$$

According to this relation, a cluster has nearly 20 atoms under such conditions, but it should be taken into consideration that the number of such clusters is rather small (less than 2% [17]) and the jet consists mainly of single atoms.

III. RESULTS AND DISCUSSION

A. Experimental results

Figures 2 and 3 show (in relative units) spectral dependencies of differential PBS cross sections for gas and cluster Xe targets, respectively, measured in the photon energy range 80–180 eV. For the data of Fig. 2, the calculated density of the gas target was 10^{15} atoms/cm^3 [18]. The data of Fig. 3 were obtained for the average number of atoms in a cluster being equal to $\sim$8500. The solid and dashed lines in these figures show the results of our model calculations, which are discussed hereafter. Some narrow characteristic lines corresponding to the $4p^5 4d^9 \rightarrow 4d^8$ radiative transition in Xe ions contribute to the experimental spectra in the region 80–90 eV [3]; the most intense line is clearly seen at the photon energy 83.5 eV.

For clusters, the PBS cross-section maximum is shifted by $\approx$10 eV to the low-energy side of the spectrum and has a full width at half maximum (FWHM) smaller than that observed for free atoms. The error in determining the positions

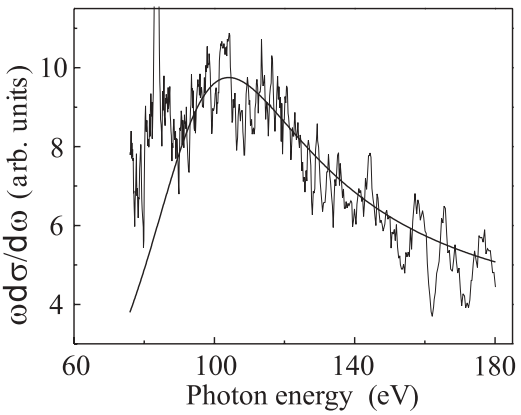

FIG. 2. Spectral dependencies of differential PBS cross section $\omega\frac{d\sigma}{d\omega}$ for 0.7-keV electrons scattered by Xe atoms. The solid curve is the model calculation of PBS cross section performed by taking into account the dielectric permeability of the emitting dipole's environment.

of the maxima is $\approx$2% for various experimental series. At the same time, for the gas and clusters, the PBS maximum is asymmetric. We would like to note that Fig. 3 reports our first observation of PBS from dielectric clusters.

Figure 4 shows the dependence of reduced FWHM of the PBS cross-section profile on Xe cluster size. To obtain the FWHM value, the experimental spectra were fitted in the spectral range 80–180 eV by an asymmetric extreme function. The obtained values were normalized by dividing them by the FWHM value of the PBS maximum from an atomic target.

Vertical error bars show the discrepancy in the experimental data measured at constant T_0 and P_0. Horizontal error bars show the error in determining the cluster size arising from inaccuracies in the exponential powers used in the Hagena equation [16].

As can be seen from Fig. 4, the FWHM of the PBS cross-section profile is weakly dependent on cluster size up to

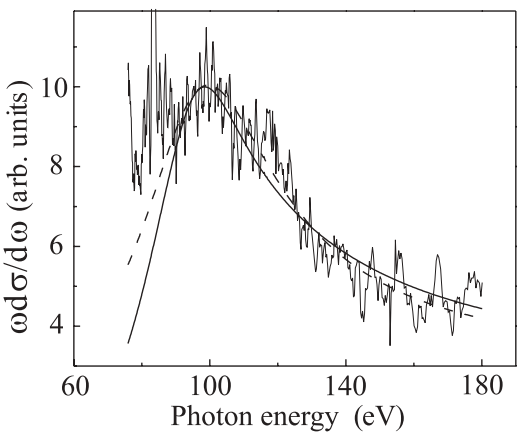

FIG. 3. Spectral dependencies of differential PBS cross section $\omega\frac{d\sigma}{d\omega}$ 0.7-keV electrons scattered by solid Xe clusters. Solid curve, model calculation of PBS cross section performed by taking into account the dielectric permeability of the emitting dipole's environment; dashed curve, model calculation of the PBS cross section performed by taking into account the frequency dependence of damping of the emitting dipole in a medium.

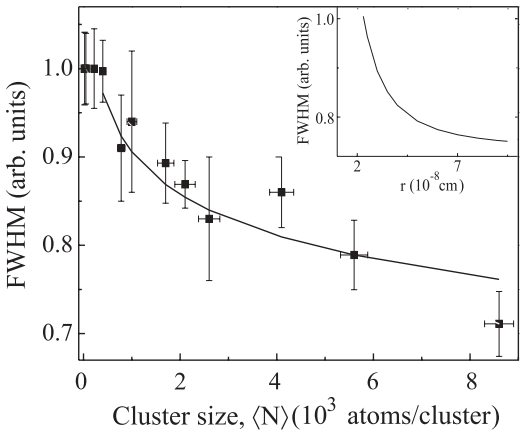

FIG. 4. Dependence of the reduced FWHM of PBS cross-section profile on Xe cluster size. ■, experimentally obtained values; solid curve, interpolated experimental data. The inset shows the calculated dependence of PBS cross section profile half-width on the Onsager parameter r.

the value of 200–300 atoms/cluster (the characteristic cluster diameter being ~30 Å). However, for clusters containing more than ~500 atoms/cluster, the PBS profile FWHM begins to decrease rather sharply with a tendency toward further saturation. For clusters with $\langle N\rangle = 8.5 \times 10^3$ atoms/cluster (the characteristic cluster diameter being ~100 Å), the decrease in FWHM is ~30%. We would like to note that the strong decrease in the PBS cross-section profile FWHM is observed for $\langle N\rangle$ values at which a diffused structural transition occurs in Xe clusters from a multilayer icosahedral to the fcc structure with deformation-type stacking faults [19].

For the electron energy of ~0.7 keV used in our experiments, the penetration depth of electrons into solid xenon is about 90 Å [20]. Thus, for the whole range of cluster sizes studied, electrons can in fact excite all of the cluster volume. For very large clusters, the PBS cross-section profile FWHM and some other spectral characteristic parameters are expected to be independent of cluster size.

B. Model calculation of the spectra

To describe the measured PBS spectra, we performed model calculations of PBS cross section for an emitting center placed in a rarefied gas or in a solid-state environment of Xe atoms. The environment was considered to be a medium with a certain dielectric permeability. For the solid-state case, an additional calculation of PBS spectra was made to take account of the retardation effect that takes place in the interaction of a damped oscillator with the surrounding atoms.

Our considerations were as follows. It is known that the cross section of the PBS on electron scattering by an atom is related to the isolated atom polarizability in such a way [4]:

$$\left[\omega\frac{d\sigma(\omega)}{d\omega}\right] = \frac{A\omega^4}{\pi v^2 e^2}\,|\alpha(\omega)|^2\left[1+\mu\ln\left(\frac{v^2}{\omega^2 R_a^2}\right)\right], \qquad (8)$$

where $\alpha(\omega) = \alpha(\omega)_{\mathrm{Re}} + i\alpha(\omega)_{\mathrm{Im}}$ is the complex polarizability of the atom, $A = e^2/c \approx 1/137$, v is the velocity of the incident electron, $\mu = \omega/mv^2$, and $R_a \sim 0.4$ Å is the effective radius of the $4d$ subshell of xenon.

According to the optical theorem, the imaginary part of the polarizability $\alpha(\omega)_{\mathrm{Im}}$ is related to the absorption cross section of an isolated atom:

$$\sigma(\omega)^a_{\mathrm{abs}} = \frac{4\pi\omega}{c}\alpha(\omega)_{\mathrm{Im}}. \qquad (9)$$

We would like to note that the giant photoabsorption resonance in xenon corresponding to the dynamic atom polarizability arises from the $4d-\varepsilon f$ transition lying above the ionization limit of the $4d$ subshell (≈70 eV). The absorption resonance profiles were measured for gaseous and solid xenon. It was demonstrated that there is little difference between the profiles [21].

Atom polarizability can be presented as follows [22]:

$$\alpha(\omega) = \alpha(\omega)_{\mathrm{Re}} + i\alpha(\omega)_{\mathrm{Im}} = \frac{B}{\omega_0^2 - \omega^2 - i\gamma\omega}, \qquad (10)$$

where ω_0 and γ correspond to the maximum position and the width of the absorption resonance, respectively, and V is an absorption amplitude parameter.

The absorption cross section depends on whether the atom is in the gaseous or solid-state environment due to the influence of the environment. Therefore, the absorption cross section $\sigma(\omega)^{\mathrm{solid,gas}}_{\mathrm{abs}}$ for a solid or a gas can be deduced from the expression obtained in Ref. [23],

$$\sigma(\omega)^{\mathrm{solid,gas}}_{\mathrm{abs}} = \left[\frac{1}{2\sqrt{2}\pi\rho\alpha(\omega)_{\mathrm{Im}}}\sqrt{\sqrt{\varepsilon'(\omega)^2+\varepsilon''(\omega)^2}-\varepsilon'(\omega)}\right]\sigma(\omega)^a_{\mathrm{abs}}, \qquad (11)$$

where ρ is the density while ε' and ε'' are the real and imaginary parts of the dielectric permeability of the medium.

To relate the dielectric permeability of the medium to the polarizability of an isolated atom, we used the following relation of the Onsager model (see, for example, Refs. [23,24]):

$$\varepsilon(\omega) = 1 + 4\pi\rho\alpha(\omega)\frac{3\varepsilon(\omega)}{2\varepsilon(\omega)+1-2[\varepsilon(\omega)-1]\alpha(\omega)/r^3}, \qquad (12)$$

where r is a parameter that characterizes the change in polarizability of an atom on placing it from a vacuum into a medium. (For the critical value $r_0^3 = (4\pi\rho/3)^{-1}$, the known Clausius-Mosotti relation [24] is valid, which does not take into account the change in polarizability.) After having performed calculations according to the Eqs. (9)–(12), one can find the PBS cross section for atoms placed in a medium by using relation (8):

$$\left[\omega\frac{d\sigma(\omega)}{d\omega}\right]^{\mathrm{solid,gas}} = \frac{16\pi A\omega^2}{c^2v^2e^2}\left[\sigma(\omega)^{\mathrm{solid,gas}}_{\mathrm{abs}}\right]^2 \times\left\{1+\left[\frac{\alpha(\omega)_{\mathrm{Re}}}{\alpha(\omega)_{\mathrm{Im}}}\right]^2_{\mathrm{solid,gas}}\right\}\left[1+\mu\ln\left(\frac{v^2}{\omega^2R_a^2}\right)\right]. \qquad (13)$$

When an isolated atom is placed in a medium, its polarizability changes; however, if the change is small we can expect the following relation to hold true:

$$\left[\frac{\alpha(\omega)_{\mathrm{Re}}}{\alpha(\omega)_{\mathrm{Im}}}\right]_{\mathrm{solid,gas}} = \left[\frac{\alpha(\omega)_{\mathrm{Re}}}{\alpha(\omega)_{\mathrm{Im}}}\right]_{a}.$$

According to the experimental data of Ref. [21], the parameters of the absorption resonance corresponding to the $4d-\varepsilon f$ transition were taken as follows: $\omega_0 = 95$ eV and $\gamma = 55$ eV. The energy of incident electrons was 0.7 keV. The solid curve in Fig. 2 shows in relative units the results of the PBS cross section calculation performed according to Eq. (13) for a rarefied Xe gas ($\rho = 1 \times 10^{17}$ cm^{-3}, $r = 1.4 \times 10^{-6}$ cm). A further decrease in gas density does not lead to any change in the PBS spectral profile. As one can see in Fig. 2, the model curve fits well the PBS cross-section profile measured for gas. The calculated PBS spectrum is shifted to higher photon energies by approximately 10 eV with respect to the $4d-\varepsilon f$ photoabsorption resonance. The first observation of the experimental PBS spectrum shift in the case of atomic xenon was reported in Ref. [2].

The solid curve in Fig. 3 shows in relative units the PBS cross section calculated for solid xenon within the above model. The model curve was obtained by using Eq. (13) with the following parameters: $\rho = 1.7 \times 10^{22}$ cm^{-3} (density of solid xenon at 50 K) and $r = 1 \times 10^{-7}$ cm (Onsager parameter). As can be seen, the model curve fits the experimental PBS spectrum measured for clusters rather well.

The above method was also employed to describe the observed effect of PBS band narrowing upon an increase in cluster size (see Fig. 4). The density of the medium was assumed to be weakly dependent on cluster size and equal to $\rho = 2 \times 10^{22}$ cm^{-3} (the critical value is $r_0 = 2.3 \times 10^{-8}$ cm). This approximation is justified by the fact that for clusters containing more than 500 atoms their density remains rather constant with further cluster size increase. Strong changes in density are only observed in small clusters ($\langle N \rangle$ being a few hundred atoms per cluster) when the contribution of less dense surface layers is rather substantial.

To describe the effect of PBS maximum narrowing at a constant cluster density, we varied the Onsager parameter r. As shown in Ref. [24], for condensed inert media the Onsager relation (12) holds for $r > r_0$. For $r \gg r_0$, the Onsager correction to the Clausius-Mosotti relation reaches its maximum value and is no longer dependent on r. The inset of Fig. 4 shows our calculated dependence of FWHM of the PBS profile on the Onsager parameter for r values from 2.3×10^{-8} to 9.5×10^{-7} cm. As can be seen in Fig. 4, the calculated dependence is in good qualitative and quantitative agreement with the experimentally obtained dependence of FWHM on average cluster size $\langle N \rangle$.

Consider now another approach to the analysis of the measured spectra which is more general and does not require any specification of the inter-relation between dielectric permeability and photoabsorption cross section on the one hand and atomic polarizability on the other. As we have already noted, PBS arises due to oscillations of the dipole moment of an atom induced by the alternating field of the incident electron. If the atom is placed in a medium, the dipole should interact with its environment to give rise, due to the retardation effect, to a frequency dependence of the damping of dipole oscillations. This physical situation is in many aspects similar to that arising when we consider dipole-like exciton excitations that interact with the phonon dissipative system in a solid [25]. For our case, following this reasoning we can take relation (8) as the basis for the calculations and assume the damping coefficient $\gamma(\omega)$ in the atom polarizability relation (10) to have a Lorentzian-like frequency dependence:

$$\gamma(\omega) = \frac{D}{(\omega_\gamma - \omega)^2 + C^2}, \tag{14}$$

where D and C are constants.

The dashed line in Fig. 3 shows the PBS cross section calculated in the framework of the above approach for $\omega_\gamma = 80$ eV, and the constants are chosen so that the ratio D/C^2 should be equal to 45 eV for the maximum value of $\gamma(\omega)$.[1] For these parameter values, the photoabsorption cross section calculated according to relations (9), (10), and (14) still has its maximum at 95 eV and is characterized by a half-width which differs little from that of the cross section calculated from the dielectric constant by using relation (11). As can be seen from Fig. 3, the latter approach provides good agreement with the experimental spectra of PBS on scattering of electrons by Xe clusters.

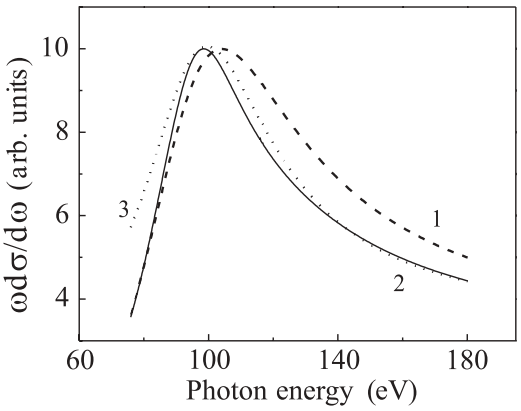

FIG. 5. Calculated PBS cross sections $\omega\frac{d\sigma}{d\omega}$: 1, calculation performed by taking into account the dielectric permeability of the emitting dipole's environment for the case of a Xe rarefied gas; 2, calculation performed by taking into consideration the dielectric permeability of the emitting dipole's environment for the case of Xe clusters; and 3, calculation performed by taking into consideration the frequency dependence of damping of the emitting dipole in a medium.

[1]Generally speaking, the damping relation (14) can be obtained by considering the oscillator equation in a medium and employing a memory function to express the summand that describes the oscillator damping. The memory function formalism takes into account the retardation effect that takes place when an oscillator interacts with a medium. For example, this can be done in the framework of the Mori equation (see, e.g., Ref. [26]). In that case, constants B and C have some physical interpretation, which is not discussed here. We would like only to note that to have good agreement with the experiment the constant C should be greater than 100 eV.

Figure 5 shows simultaneously the PBS cross-section calculation results for a rarefied gas (curve 1) and those for clusters (obtained within the two approaches considered above) in order to facilitate comparison between the data. These curves have already been presented separately in Figs. 2 and 3. The two model curves that fit the PBS spectrum from clusters are very close to each other. It can also be seen that for a cluster target there is a shift in PBS maximum position of about 10 eV to the lower-frequency side of the spectrum compared to that for a gaseous target. In addition, the FWHM of the PBS cross-section profile for the clusters is narrower by ~20% than that for the gas (the difference in areas under the PBS curves is ~30%).

IV. CONCLUSIONS

The paper reports the results of comparison experiments on PBS that arise from the scattering of electrons by gaseous and solid xenon. The measurements were made in the photon energy range 80–180 eV. Gas and cluster supersonic jets were used as the targets; in the latter case, the number of atoms in a cluster was varied from several tens to 8.5×10^3. It was found that the PBS maximum shifts toward lower photon energies (by ~10 eV) and narrows upon passage from the gaseous to the cluster target. The strongest narrowing was observed upon an increase in atom number for clusters having more than 500 atoms (up to almost 30% for $\langle N \rangle = 8.5 \times 10^3$ atoms/cluster; the cluster diameter was ~100 Å).

Model calculations of PBS spectra were performed for gaseous and solid xenon. The calculated curves fit the measured PBS spectra well and reproduced the spectral changes observed upon transition from gas to cluster targets. The calculations were made within two approaches applied to describe PBS. According to one approach, the gaseous or solid medium was characterized by a complex dielectric permeability which was related to atomic polarizability that determines the PBS spectrum by using the Onsager formula. This approach made it possible to describe the spectra and demonstrate that the PBS cross-section profile narrowing is due to an increase in the Onsager parameter with increasing number of atoms in a cluster. Good agreement of the model calculations taking into account dielectric permeability with the experimental data allows us to conclude that there is a noticeable influence of the solid-state cooperative effect on PBS spectra formation in a cluster. Since the Onsager parameter describes the contribution of two- and three-particle interactions to dielectric permeability, their total effect becomes greater as atom number increases in a cluster.

According to the other approach used to model the PBS spectra, it was taken into account that there must be some retardation effect for a dipole emitting in a solid-state environment due to its interaction with the environment. This was done by introducing a frequency dependence of the dipole damping. This approach is more general and does not require the use of dielectric permeability. Within this approach too it was possible to describe the experimental PBS spectra. This provides some additional evidence that PBS spectra are highly sensitive to cooperative effects, including possibly those arising from resonance dipole interactions in solid-state matter.

ACKNOWLEDGMENTS

The authors are grateful Dr. V. L. Vakula for assistance in preparing the paper.

[1] *Polarization Bremsstrahlung of Particles and Atoms*, edited by V. N. Tsytovich and I. M. Oiringel (Plenum, New York, 1992).
[2] E. T. Verkhovtseva, E. V. Gnatchenko, and P. S. Pogrebnjak, J. Phys. B **16**, L613 (1983).
[3] E. T. Verkhovtseva, E. V. Gnatchenko, P. S. Pogrebnjak, and A. A. Tkachenko, J. Phys. B **19**, 2089 (1986).
[4] E. T. Verkhovtseva, E. V. Gnatchenko, B. A. Zon, A. A. Nekipelov, and A. A. Tkachenko, Zh. Eksp. Teor. Fiz. **98**, 797 (1990) [Sov. Phys. JETP **71**, 443 (1990)]; E. T. Verkhovtseva and E. V. Gnatchenko, Low Temp. Phys. **28**, 270 (2002).
[5] S. Portillo and C. A. Quarles, Phys. Rev. Lett. **91**, 173201 (2003).
[6] E. V. Gnatchenko, A. A. Tkachenko, and A. N. Nechay, Pis'ma Zh. Eksp. Teor. Fiz. **86**, 344 (2007) [JETP Lett. **86**, 292 (2007)].
[7] V. S. Vukstich, Yu. V. Zhmenyak, and I. P. Zapesochnyi, Abstracts of the 13th International Conference on the Physics of Electronic and Atomic Collisions (Berlin), 745 (1983).
[8] T. M. Zimkina, I. I. Lyakhovskaya, A. S. Shulakov, V. I. Alaverdov, and V. I. Rasuvaeva, Fiz. Tverd. Tela (Leningrad) **25**, 26 (1983).
[9] T. M. Zimkina, A. S. Shulakov, A. P. Braiko, A. P. Stepanov, and V. A. Fomichev, Fiz. Tverd. Tela (Leningrad) **26**, 1981 (1984).
[10] A. G. Lyalin and A. V. Solov'yov, Radiat. Phys. Chem. **75**, 1358 (2006).
[11] L. I. Kurkina, Phys. Solid State **46**, 557 (2004).
[12] V. A. Astapenko, Zh. Eksp. Teor. Fiz. **128**, 88 (2005) [JETP **101**, 73 (2005)].
[13] M. Ya. Amusia, T. M. Zimkina, and M. Yu. Kuchiev, Zh. Tekh. Fiz. **52**, 1424 (1982).
[14] E. V. Gnatchenko, A. N. Nechay, and A. A. Tkachenko, Phys. Rev. A **80**, 022707 (2009).
[15] O. F. Hagena, Rev. Sci. Instrum. **63**, 2374 (1992).
[16] A. G. Danylchenko, S. I. Kovalenko, and V. N. Samovarov, Pis'ma Zh. Tekh. Fiz. **34**, 87 (2008).
[17] P. A. Skovorodko, in *Rarefield Gas Dynamics*, edited by O. M. Belotserkovskii, M. N. Kogan, S. S. Kutateladze, and A. K. Rebrov (Plenum, New York, 1985).
[18] P. A. Skovorodko, Ph.D. thesis, Institute of Thermophysics, Novosibirsk, 1977.
[19] E. T. Verkhovtseva, S. I. Kovalenko, D. D. Solnyshkin, and E. A. Bondarenko, Low Temp. Phys. **23**, 140 (1997)
[20] A. Adams and P. K. Hansma, Phys. Rev. B **22**, 4258 (1980).
[21] R. Haensel, G. Keitel, P. Schreiber, and C. Kurtz, Phys. Rev. **188**, 1375 (1969).
[22] U. Fano and J. W. Cooper, Rev. Mod. Phys. **40**, 441 (1968).
[23] X.-G. Ma, Phys. Lett. A **348**, 310 (2006).
[24] O. G. Bokov and Yu. I. Naberukhin, J. Chem. Phys. **75**, 2357 (1981).
[25] A. S. Davydov, *Theory Solid State* (Nauka, Moscow, 1976).
[26] A. Abragam and M. Goldman, *Nuclear Magnetism: Order and Disorder* (Clarendon, Oxford, 1982).